Retinex-based Visual Image Enhancement Algorithm for Coal Mine Exploration Robots

Dong She
College of Computer and Art, Anhui Technical College of Industry and Economy, Hefei 230051, China
E-mail: sd1203001@126.com

Keywords: Retinex theory; Image enhancement; Attention mechanism; Convolutional neural network; Generate adversarial networks

Received: April 10, 2024

Due to the unique nature of coal mining environments, images captured in low illumination environments often have problems like low brightness, poor contrast, and loss of detail information, which seriously affects the quality of images and the information carried. In response to this issue, this study proposes a visual image enhancement algorithm for coal mine exploration robots based on Retinex. This method first decomposes low illumination images into light mapping and reflection mapping through the light smoothing loss function, and then enhances the former and denoises the latter through an improved Retex-net. Finally, the two are combined to output the enhanced image. The conclusion verified that when the training set reached 1000, the structural similarity values of the improved Retinex-Net algorithm, global illumination perception and detail preserving network, relative average generative adversarial network, and Retinex-Net were 0.98, 0.95, 0.89, and 0.88, respectively. When the iterations were 500, the accuracy of Retinex-Net algorithm, global illumination perception and detail preserving network, relative average generative adversarial network, and Retinex-U-Net algorithm were 0.78, 0.53, 0.38, and 0.31, respectively. The data indicates that the designed algorithm owns good performance and makes a positive contribution to improving the efficiency and safety of coal mine exploration work.

Povzetek: Razvit je nov algoritem za izboljšanje kvalitete slik za raziskovalne robote v rudnikih premoga, ki temelji na Retinex teoriji. Gre za obdelavo slik v slabo osvetljenih okoljih, kar izboljšana jasnost in kontrast slik prispevata k večji učinkovitosti in varnosti pri raziskovanju rudnikov.

1 Introduction

With the growth of the economy and social progress, people can obtain a large amount of information through images and transmit information through digital images. Digital images are the medium for information transmission. Due to the distinctive characteristics of coal mining environments [1], robots frequently encounter challenges such as uneven illumination and low contrast in images obtained in complex mine environments. These issues significantly impact the clarity and usability of the images [2]. Therefore, how to improve the image quality obtained by robots has become one of the hotspots in the research of coal mine exploration robot technology. In response to the issue of image quality in coal mine exploration robots, this study proposes a Retinex-based visual image enhancement algorithm (IEA) for coal mine exploration robots. Retinex algorithm is a classic IEA mainly used to strengthen the brightness and contrast of images while maintaining the details. This algorithm can effectively compensate for uneven illumination by simulating the human eye's perception mechanism of light, enabling the image to maintain high clarity and visibility in complex environments. The research content has five parts. The first part briefly introduces the other scholars' research topics on visual IEA. The second part is a review of the main methods used in this study. The third part is to study the model results obtained through the application of methods and analyze the results. The fourth part is a discussion of the research results. The fifth part is a summary of all the above studies and prospects for future research.

2 Related works

As a carrier of information, images play an important role in various fields. Fu et al. found that many existing methods in the process of weak light image enhancement cannot effectively handle noise, resulting in color deviation and overexposure issues. Moreover, in the absence of paired data, existing methods could not guarantee that quality. In response to this, the team proposed an unsupervised low light image (LLI) enhancement network. The results indicated that this network could enhance LLIs and solve problems such as noise and color deviation [3]. Xu et al. found that information in LLIs is difficult to capture, so they designed a multi-scale fusion framework for LLI enhancement. This method generated exposure images through a remapping function, then selected different indicators as weight maps, and finally integrated the

frequency bands of the images. It could keep the detailed information of the image without causing color distortion [4]. Zhou et al. found that the clarity of outdoor images can be reduced due to haze, and put forward a single IEA built on weighted guidance coefficients for dark channel prior and joint adaptive image enhancement. This method could enhance images under haze weather to restore the original information of the image. This study showed that the proposed method addressed the issues of image distortion and loss of detail information, and had higher efficiency than traditional IEA [5].

He et al. found that in low illumination or haze weather, images taken outdoors have issues such as color distortion, missing details, and poor imaging quality. They proposed a method for image enhancement combined with adaptive color restoration and detail preservation. It restored the color of the image through multi-channel fusion, and then enhanced the details through a method based on detail preservation. This method could enhance the recognition of low illumination images (LII) [6]. Zhang et al. found that traditional IEAs can lead to local over enhancement and noise amplification when strengthening images. Therefore, a method for infrared image enhancement using local entropy mapping histogram adaptive segmentation has been proposed. This method could enhance images and maintain good details, leading traditional IEAs in quantitative evaluation [7]. Lu et al. found that images captured under low light conditions usually display issues like insufficient brightness and severe noise. They proposed a channel segmentation attention network that can distinguish the information contained in features through attention modules. The proposed method has been proven to better suppress chromaticity differences while enhancing LII [8].

In summary, many scholars have conducted research on LLI enhancement and have achieved certain results. Although these studies have made some progress in image enhancement, there are still some limitations, including lack of data, algorithm complexity, parameter sensitivity, universality, and consideration of practical application scenarios. Furthermore, they fail to acknowledge that illumination in complex environments is not uniform, which results in enhanced images that do not accurately reflect the information present. This study proposes a visual IEA for coal mine exploration robots based on Retinex. This method first decomposes LII into illumination maps and reflection maps through the illumination smoothing loss function (LF). Then, by improving Retinex-Net, the two are combined to output the enhanced image. This way can enhance LII and preserve the original information, reducing noise information. A detailed literature comparison is shown in Table 1.

Table 1: Summary table

Authors	Year	Method	Key results	Limitations
Fu et al [3].	2022	Unsupervised LLI Enhancement Network	Effectively enhances LLI, addresses noise and color deviation issues.	Lack of paired data, general applicability in various scenarios not discussed.
Xu et al [4].	2021	Multi-scale Fusion Framework for LLI Enhancement	Preserves detailed information without color distortion, integrates frequency bands effectively.	Limited discussion on computational complexity, potential challenges in real-time applications not addressed.
Zhou et al [5].	2021	Single IEA with Weighted Guidance Coefficients	Enhances images under haze weather, restores original information, addresses image distortion and loss of detail information.	Lack of extensive comparison with other methods, potential sensitivity to parameter tuning.
He et al [6].	2021	Image Enhancement with Adaptive Color Restoration	Combines adaptive color restoration and detail preservation, enhances recognition of LIIs, restores color and enhances details effectively.	Lack of discussion on computational efficiency, potential issues with generalization to diverse datasets not addressed.

Zhang et al [7].	2022	Infrared Image Enhancement with Local Entropy Mapping	Enhances images while maintaining good details, surpasses traditional IEAs in quantitative evaluation.	Potential sensitivity to parameter settings, lack of discussion on real-world applicability.
Lu et al [8] .	2022	Channel Segmentation Attention Network	Suppresses chromaticity differences while enhancing LIIs, distinguishes information through attention modules effectively.	Computational overhead not discussed, potential challenges in training on large-scale datasets not addressed.

3 Retinex-based Visual IEA

The first section of this chapter first explains the Retinex theory, and then introduces Retinex-Net through this theory and models it using this method. The second section introduces attention mechanism and U-shaped neural network to perfect the model based on the first section.

3.1 Uniformly illuminated image enhancement based on retinex for coal mine exploration robot vision

Retinex theory is a theory about visual perception, mainly exploring how humans perceive color and brightness. The core viewpoint of this theory is that human visual perception is not only dependent on the photoreceptor cells of the eye, but also influenced by the processing and interpretation of the brain [9]. In accordance with this, the observed color of an object is determined by the reflected wavelength and is not related to the intensity of light. The calculation theory is shown in Figure 1.

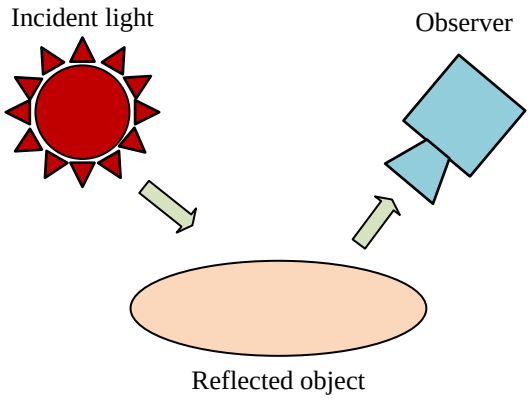

Figure 1: Retinex theoretical model diagram

In Figure 1, the incident light emits photons, illuminates the surface of the object, and reflects them into the human eye, forming an image in the human eye. This process can be expressed through a formula, as shown in equation (1).

$$S(x,y) = I(x,y) \circ R(x,y) \quad (1)$$

In equation (1), $S(x,y)$ is the imaging of the observer. $I(x,y)$ means the incident light image. $R(x,y)$ represents reflectivity. It is an inherent property of an object. The incident image represents the intensity of light. Reflectivity represents the ability of light to reflect. This study is based on Retinex theory and convolutional neural networks (CNN), and proposes an improved Retinex-Net and illuminance smoothing based uniform illumination IEA for LII. The Retinex-Net is divided into three parts, namely the decomposition part, the adjustment part, and the reconstruction part [10]. Among them, the decomposition part is composed of a 5-layer CNN structure. It inputs LII into a decomposition network, analyzes and processes the images, and outputs the reflection and illumination components of the images. Then, the output image is input into the enhancement network. The Enhanced Network is a 9-layer CNN structure. This structure adjusts the illumination image to

maintain overall consistency in the photo, and uses multi-scale connections to crop local distributions. At the same time, multi-scale cascading technology is introduced to adjust illumination from a multi-scale perspective. Its pseudocode is shown in Figure 2.

```
Pseudocode: Retinex-Net Clustering Algorithm

Function Retinex_Net_and_Illuminance_Smoothing(image):
    reflected_component, illuminance_component = Decomposition_Net(image)

    adjusted_illuminance = Enhancement_Net(illuminance_component)

    enhanced_image = Reconstruction(reflected_component, adjusted_illuminance)

    return enhanced_image

function Decomposition_Net(image):
    CNN_layers = define_CNN_layers()

    reflected_component = CNN_layers(image)
    illuminance_component = image - reflected_component

    return reflected_component, illuminance_component

function Enhancement_Net(illuminance_component):
    CNN_layers = define_CNN_layers()

    adjusted_illuminance = CNN_layers(illuminance_component)

    return adjusted_illuminance

function Reconstruction(reflected_component, adjusted_illuminance):
    enhanced_image = reflected_component + adjusted_illuminance

    return enhanced_image
```

Figure 2: Retinex-Net pseudocode

Due to the greater noise in dark areas of the image, the noise will also increase during the enhancement process. Therefore, it is necessary to use denoising operations to denoise the image. In the low illumination IEA built on Retinex-Net, the LF is composed of the weighted sum of the decomposition and the enhancement networks. The decomposition network is responsible for decomposing LIIs into reflection and illumination components, usually a structure composed of multi-layer CNNs. This network decomposes the input LII into reflection and illumination components through learning. The reflection component represents the detailed information in the image, while the illumination component represents the global illumination situation of the image. By decomposing the network, the system can separate global illumination information and detail information in the image. This makes it easier for the system to process LLIs, as under low light conditions, the changes in global illumination are usually significant, while the details are relatively more stable. The illumination components output by the network are enhanced and decomposed by the network, adjusted to improve image quality and minimize noise. A typical structure is a multi-layer CNN that receives illumination components from the decomposition network as input and then learns to adjust the illumination components to maintain overall consistency of the photo, reduce noise, etc. The main task of enhancing the network is to adjust the illumination of the image based on the illumination components provided by the decomposition network to improve the quality of the image. In this process, the enhancement network can utilize its deep learning ability to learn the features and structure of images, thereby better processing image noise and reducing the noise introduced during the enhancement process while enhancing image brightness. The expression is equation (2).

$$\begin{cases} L_{decome} = L_{recom} + \lambda_{ir} L_{ir} + \lambda_{is} L_{is} \\ L_{recon} = \sum_{i=low,normal} \sum_{j=low,normal} \lambda_{ij} \left\| I_j R_i - S_j \right\|_1 \end{cases} \quad (2)$$

In equation (2), L_{decome} is the LF of the decomposed network, and L_{recon} is the reconstruction loss. λ_{ir} is the consistency of balanced reflectivity. L_{ir} is the refractive index loss. λ_{is} is the smoothness of illumination. L_{is} represents the smoothing loss of illumination. λ_{ij} represents the reconstruction coefficient. R is the illumination image [11]. $\| \|_1$ is the L_1-norm. I is the illuminance component. The calculation formulas for L_{ir} and λ_{is} are shown in equation (3).

$$\begin{cases} L_{ir} = \left\| R_{low} - R_{normal} \right\|_1 \\ \lambda_{is} = \sum_{i=low,normal} \left\| \nabla I_i \exp(-\lambda_g \nabla R_i) \right\| \end{cases} \quad (3)$$

In equation (3), R_{low} represents the reflection component (ReC) of the LLI. ∇ is the gradient in the horizontal and vertical ways. R_{normal} is the ReC of normal light. λ_g represents the equilibrium coefficient. Although the Retinex-Net can improve the brightness of images, it also generates a large amount of noise, and processed images can also cause color distortion. In coal mine exploration, this disadvantage is particularly evident. Therefore, this study improves the method and the improved structure is Figure 3.

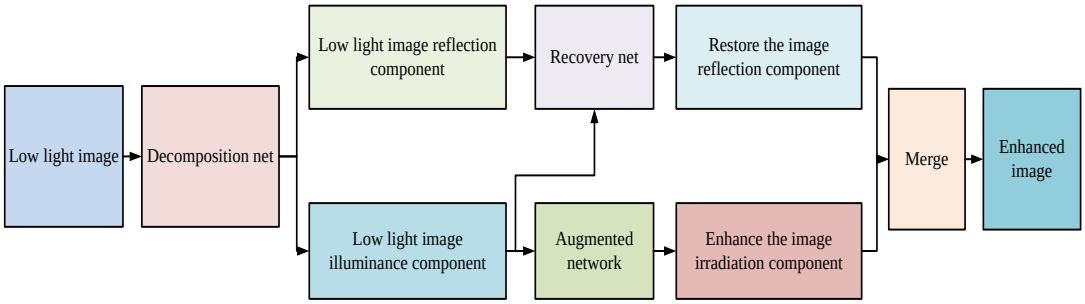

Figure 3: Network structure diagram of improved Retinex-Net algorithm

According to Figure 3, the structure has three modules: decomposition, ReC recovery, and illumination component enhancement. The LLI is input into the decomposition module, which outputs the reflection and illumination components of the LLI. Two components are input into the recovery network and the ReCs of the recovered image are output. The LLI illuminance component is input into that enhancement network, and the illuminance component of the optimized image is output. At last, the two components are fused to obtain the enhanced image [12]. To enhance the decomposition ability of the decomposition module, its LF is equation (4).

$$L_{decome} = L_{re} + \lambda_r L_r + \lambda_i L_i \tag{4}$$

In equation (4), L_{re} is the reconstruction loss value. λ_r represents the consistency coefficient. L_r is the ReC loss. λ_i represents the smoothness coefficient of the illumination. L_i is the smoothing loss value of the illuminance. The reconstruction loss is equation (5).

$$L_{re} = \left\| I_l R_l - L_l \right\|_1 + \left\| I_h R_h - L_h \right\|_1 \tag{5}$$

In equation (5), I_l and I_h, R_l and R_h represent the illuminance and ReC of the LLI and a normally illuminated image. L_l and L_h represent weak and normal light images. The expression for ReC loss is equation (6).

$$L_r = \left\| R_i - R_h \right\|_1 \tag{6}$$

As calculation of Equation (6), the smoothing loss of the illuminance component is equation (7).

$$L_i = \left\| \frac{\nabla I_l}{\max(|\nabla L_l|, \varepsilon)} \right\|_1 + \left\| \frac{\nabla I_h}{\max(|\nabla L_h|, \varepsilon))} \right\|_1 \tag{7}$$

In equation (7), ∇ represents the gradient value. ε is a positive number that tends towards zero, used to prevent the denominator from being zero. The gradient of the illumination component should be as large as possible in the flat position of the illumination component, which can increase the smoothness and make the image brightness change smoothly.

In the decomposition module, it is necessary to add constraints to the module. The most important aspect is the structural perception smoothness of illumination mapping. When the illumination component is smooth, local details and enhanced noise are preserved. It is necessary to perform denoising on the ReC before outputting the reconstructed image [13]. This study uses the ReC of the normal image output by the decomposition module as the true value and its LF is Equation (8).

$$L_{restore} = \left\| R_{re} - R_h \right\|_2^2 + \left\| \nabla R_{re} - \nabla R_h \right\|_2^2 + \lambda_c L_c \tag{8}$$

In equation (8), $\| \|_2$ represents the L_2-norm. R_{re} represents the recovered ReC. To avoid color differences between the image and the original color, and to evaluate the color of the enhanced image, the resulting color LF is equation (9).

$$L_c = \left\| R_{reb} - R_{hb} \right\|_2^2 \tag{9}$$

In equation (9), R_{reb} and R_{hb} represent the images of R_{re} and R_h after Gaussian blur, respectively. Due to the fact that the true value of the illuminance component does not exist, it is needed to build a mapping learning process between LLIs and normal images. The role of reinforcement networks is to establish the process of mapping learning. Firstly, the input image is sampled and the local illumination distribution is reconstructed from the sampled information. Then, the feature map size is adjusted to match the input image size. Then it is spliced, fed into the lower layer, and finally reconstructed with the convolutional layer to reconstruct the

illumination component. The LF of the enhancement network is equation (10).

$$L_{enhance} = \left\| I_{en} - I_h \right\|_2^2 + \left\| \nabla I_m - \nabla I_h \right\|_2^2 \quad (10)$$

In equation (10), I_{en} is the enhanced illuminance component. ∇ is the gradient value. $\| \ \|_2$ represents the L_2-norm.

3.2 Non-uniform illumination image enhancement based on retinex for coal mine exploration robot vision

In coal mine surveying, the environment most often faces uneven illumination due to the influence of weather and varying degrees of illumination. Retinex-based image enhancement cannot meet the requirements of complex environments. Therefore, based on this method, attention mechanism and U-shaped neural network (U-Net) are introduced to enable the improved Retinex algorithm model to enhance images in non-uniform illumination environments.

Attention mechanism is a method of simulating human attention, which improves the model efficiency in processing large-scale data and complex tasks through selective attention and weighted processing of input data. Attention mechanisms are widely used in the fields of machine learning and artificial intelligence. The attention mechanism could be segmented into channel, spatial, and mixed domains in terms of attention domain [14]. Channel domain refers to a method of selectively weighting different channels or feature dimensions of input data in the attention mechanism. In deep learning, input data typically has multiple channels or feature dimensions. For example, in image processing, an RGB image has three channels. By applying attention mechanisms in the channel domain, the model can dynamically adjust the level of attention to different channels or feature dimensions, thereby improving the model's extraction and utilization of important information. This method can achieve adaptive feature selection for input data in different tasks and scenarios. Its structure is Figure 4.

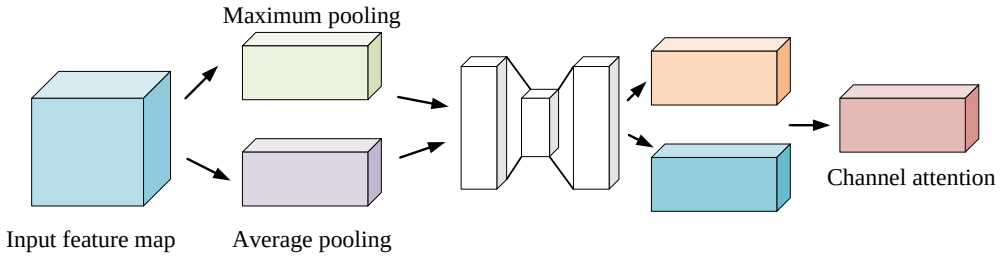

Figure 4: Channel attention module

In Figure 4, the feature map is subjected to maximum and average pooling. Then, two context descriptors are input into the shared network, and the channel attention map is gained through the shared network output. The calculation of the channel is equation (11).

$$M_c(F) = \sigma(W_1(W_0(F_{avg}^c)) + W_1(W_0(F_{\max}^c))) \quad (11)$$

In equation (11), σ is the sigmoid function. W_0 is the channel attention map. F_{avg}^c and $F_{\max}^c$ represent context descriptors for two spaces. The spatial attention concentrates more on specific positional information. Calculating spatial attention requires processing in the direction of the channel axis through average and max pooling, and then parallelizing the processing results to create an effective feature descriptor [15]. Its structure is Figure 5.

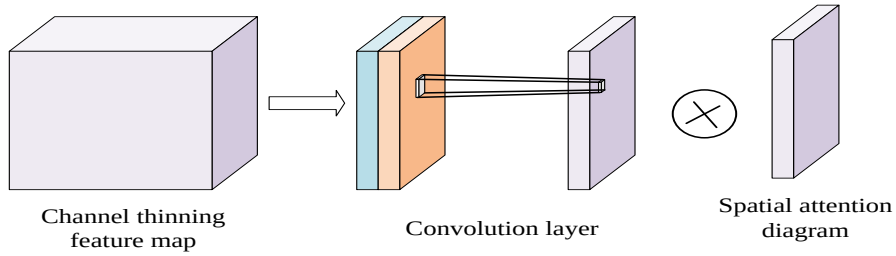

Figure 5: Spatial attention module

In this figure, the model first aggregates the channel information of feature maps through average and max pooling, thereby generating two feature images. Then these two feature images are connected and input into the network to generate a spatial attention map. The calculation formula is equation (12).

$$M_s(F) = \sigma(f^{7\times7}([F^s_{avg}; F^s_{\max}])) \tag{12}$$

In equation (12), $f^{7\times7}$ is a convolutional kernel. The convolutional attention mechanism module is a technology that combines convolutional operations and attention mechanisms to improve the performance of CNN in processing image or sequence data. This module typically includes two key components: attention mechanism and convolution operation. The former is responsible for calculating the importance weight of each channel or feature to determine which channels or features the model should focus on. The latter is responsible for feature extraction and processing of input data [16]. This module is shown in Figure 6.

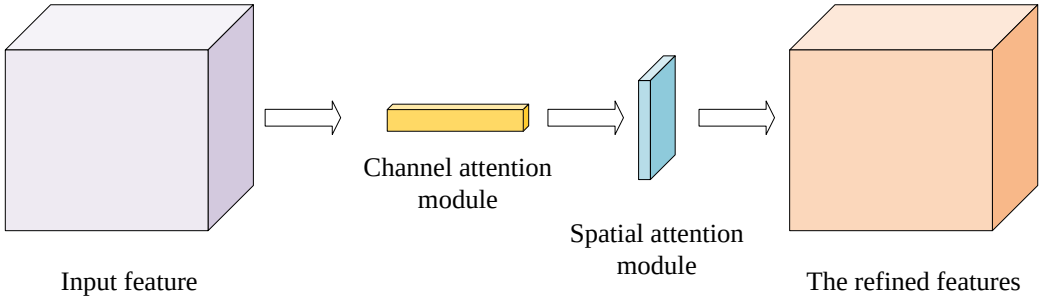

Figure 6: Convolutional attention mechanism module

According to Figure 6, features are input in this module, and local feature details are learned on the channel and spatial position feature information through the two modules [17]. Finally, the obtained features are output. The entire attention process is equation (13).

$$\begin{cases} F'' = M_s(F') \otimes F' \\ F' = M_c(F) \otimes F \end{cases} \tag{13}$$

In Equation (13), F'' means the refined feature map. $\otimes$ is element multi-plication. F' represents a feature map. Due to the characteristics of U-Net networks, U-Net is introduced into the model to denoise the reflected components. To deal with the matter of color distortion in reflected components, the product attention mechanism is added to the U-Net [18]. A LF is added to the network for constraints, as shown in equation (14).

$$\begin{cases} L_{restore} = \lambda_s L_{square} + \lambda_g L_{grod} + \lambda_c L_{color} \\ L_{square} = \left\| R_{re} - R_h \right\|_2^2 \\ L_{grod} = \left\| \nabla R_{re} - \nabla R_h \right\|_2^2 \end{cases} \tag{14}$$

In equation (14), L_{square} represents the mean square error (MSE) LF. R_{re} is the recovered ReC. λ_s is the MSE loss coefficient. λ_g represents the gradient loss coefficient. L_{color} is the color LF. λ_c represents the color perception balance coefficient. Due to the complexity of the environment, the brightness of images captured in low illumination environments is unevenly distributed. To handle the issue of excessive brightness enhancement caused by the illumination map enhancement network, improvements have been made to the illumination network, as shown in Figure 7.

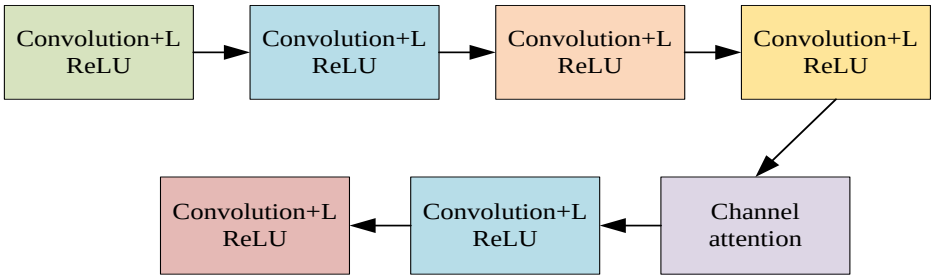

Figure 7: Improved illumination map enhancement network

In Figure 7, the network includes six convolutional layers. By adding a channel attention module to the convolutional layer and analyzing the relationship between feature channels, a channel attention map is generated to analyze illumination information [19]. The improved illuminance map enhances the network LF as shown in equation (15).

$$L_{enhance} = \left\| I_{en} - I_h \right\|_2^2 + \left\| \nabla I_{en} - \nabla I_h \right\|_2^2 \quad (15)$$

In equation (15), I_{en} represents the enhanced illuminance component. The images are reconstructed using the Retinex theoretical model. The reconstructed image is equation (16).

$$S_{enhance}(x, y) = R_{en}(x, y) \times I_{en}(x, y) \quad (16)$$

In equation (16), R_{re} represents the recovered ReC. I_{en} is the enhanced illuminance component. By combining the two, the reconstructed image can be obtained.

4 Performance analysis of visual IEA for coal mine exploration robots based on retinex

The first section of this chapter compares the performance of different models under different training and validation sets, as well as different iterations. In the second section, after comparing the performance of the model, images of the mining area are selected to test the performance of the model.

4.1 Performance analysis of uniform illumination image enhancement based on retinex

This experiment uses the LOL dataset. This dataset contains a dataset of low light enhanced images extracted from real scenes, including a variety of scene maps. The experimental hardware configuration uses Intel Core i5-8750H CPU, NVIDIA Geforce GTX2080Ti GPU, 8 GB graphics memory, and 16 GB memory. Then, the GLADNet and RAGAN are introduced to compare with the proposed algorithm, the results are shown in Figure 8.

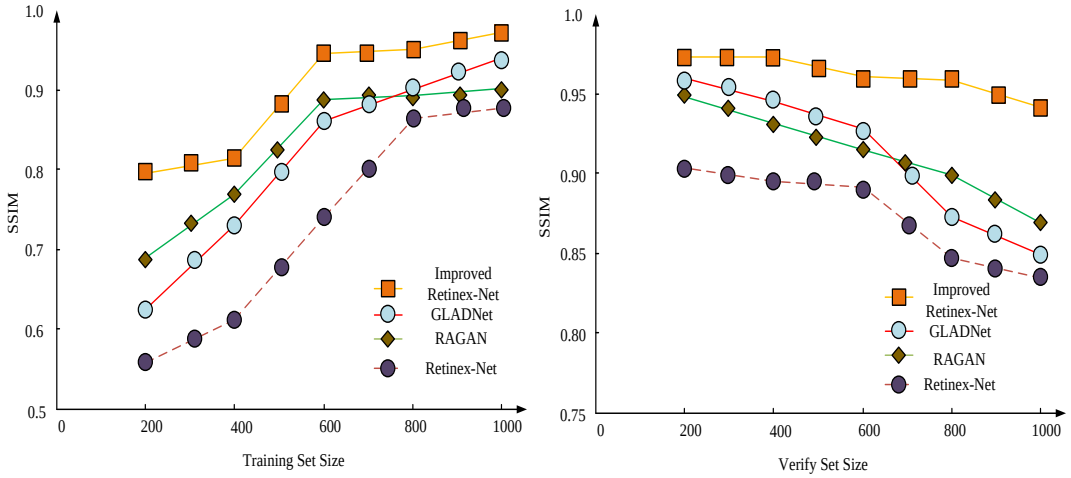

(a)Changes in accuracy of different algorithm models in training sets

(b)Changes in accuracy of different algorithm models in the validation set

Figure 8: Comparison of SSIM values for four algorithms

Figures 8(a) and 8(b) represent the Structural Similarity Index Measure (SSIM) values of the four algorithms in the training and validation sets. As the training set increases, the SSIM values of each algorithm also increase. Among them, the improved Retinex-Net algorithm tends to stabilize its performance and exhibits good performance when the quantity of training sets is around 600. When the number of training sets for other algorithms is 600, their model performance still fluctuates and is not at its optimal performance. When the training set reaches 1000, the SSIM values of the improved Retinex-Net algorithm, GLADNet, RAGAN, and Retinex-Net algorithms are 0.98, 0.95, 0.89, and 0.88, respectively. In the validation set, as the validation set increases, all three models except for the improved Retinex-Net algorithm have reduced SSIM values as the validation set increases. The improved Retinex-Net algorithm does not show significant changes as the validation set increases. The performance of the four methods is compared, and the results are shown in Figure 9.

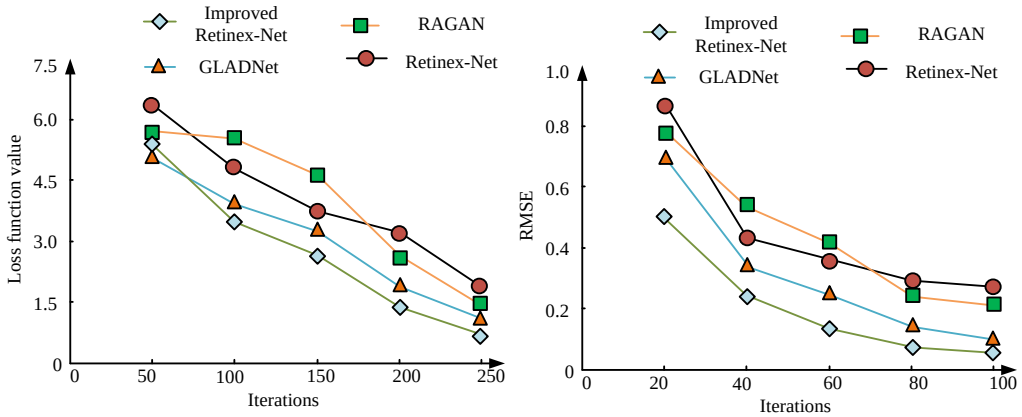

(a)Loss function values for four methods (b)RMSE for four methods

Figure 9: LF and RMSE values of four algorithms

Figures 9(a) and 9(b) represent the LF and Root Mean Square Error (RMSE) of the four algorithms, and the values of the four algorithms decrease as the iterations increase. In 9(a), the improved Retinex-Net algorithm has the greatest decrease in the LF value, while the Retinex-Net algorithm has the smallest decrease. When the iterations reach 250, the LF of the improved Retinex-Net, GLADNet, RAGAN, and Retinex-Net are 1.8, 1.5, 1.2, and 0.8, respectively. In 9(b), the RMSE of the improved Retinex-Net decreases the most. When the iterations reaches 100, the RMSE values of the improved Retinex-Net algorithm, GLADNet, RAGAN, and Retinex-Net algorithms are 0.28, 0.20, 0.11, and 0.09. The results prove that the improved Retinex-Net has high performance among the four algorithm models.

4.2 Performance analysis of non-uniform illumination image enhancement based on retinex

Retinex-based image enhancement cannot meet the requirements of complex environments, so attention mechanism and U-Net network are introduced on the basis of this method. The purpose is to enable the improved Retinex algorithm model to enhance images in non-uniform illumination environments. Their performance are compared separately, and the results are shown in Figure 10.

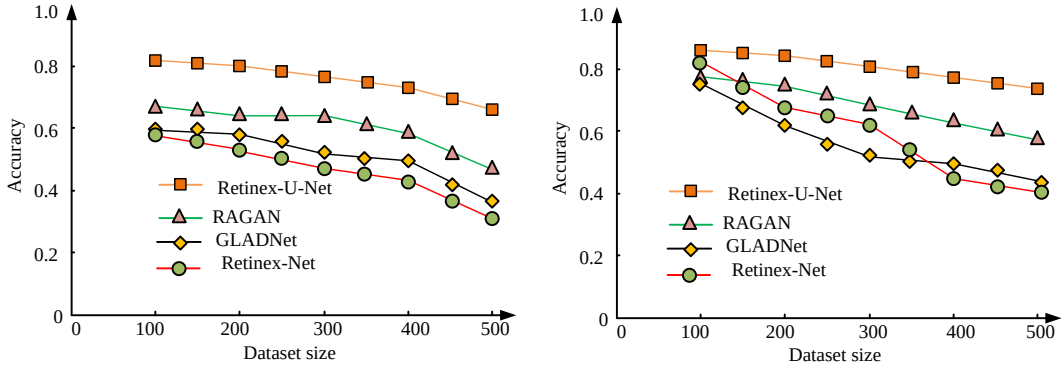

(a) LOL data (b) REALLIGH data

Figure 10: Performance comparison of four algorithms

Figure 10(a) shows the performance comparison of various algorithms in the LOL dataset, and Figure 10(b) shows the performance comparison of various algorithms in the REALLIGHT dataset. As shown in Figure 10, in both datasets, the performance of the four algorithms decreases with the increase of the dataset. However, the Retinex-U-Net algorithm model does not show a significant decrease in performance with the increase of the experimental set and remains at a high level. The algorithm performance of Retinex-Net, GLADNet, and RAGAN has significantly decreased. When the number of iterations is 500, the accuracies of Retinex-Net algorithm, GLADNet, RAGAN, and Retinex-U-Net algorithm are 0.78, 0.53, 0.38, and 0.31, respectively. The experimental results show that the Retinex-U-Net algorithm model has good recognition accuracy for larger datasets, and shows good model accuracy among the four models. Performance analysis of ores and ordinary stones

in the mining area is conducted under different iteration times, and the results are shown in Figure 11.

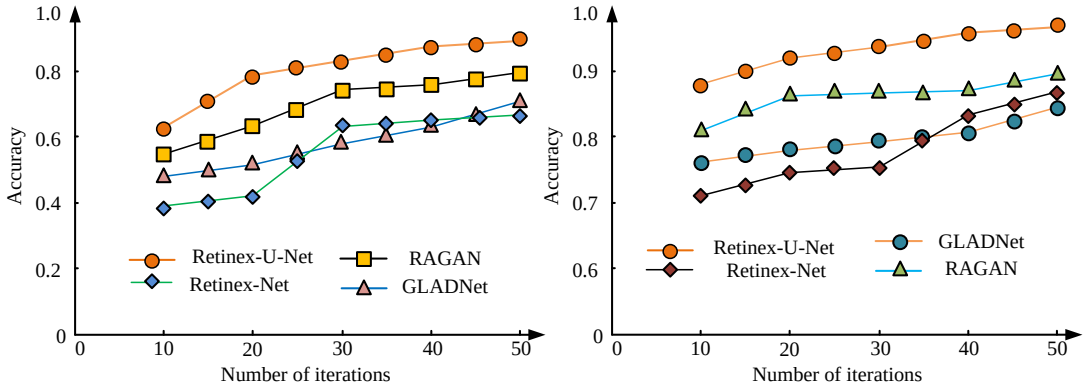

(a)Four algorithms to enhance the performance of ore pictures

(b)Four algorithms to enhance the performance of ordinary stone pictures

Figure 11: Enhancement effect of various algorithms on images of ores and ordinary stones

Figures 11(a) and 11(b) show the enhancement performance of four methods on images of ores and ordinary stones. In 11(a), as the iterations increase, the model performance for ore images also increases. When the iterations reach around 30, the performance of the Retinex-U-Net algorithm basically reaches its maximum, and the performance of other models does not reach its maximum. In 11(b), the enhancement performance of ordinary stones is basically consistent with that of ores. When the number of iterations reaches around 30, the performance of the Retinex-U-Net algorithm model reaches its maximum. This indicate that the Retinex-U-Net algorithm can achieve good model performance with fewer iterations. Common items in the mining area are selected to enhance them, as shown in Figure 12.

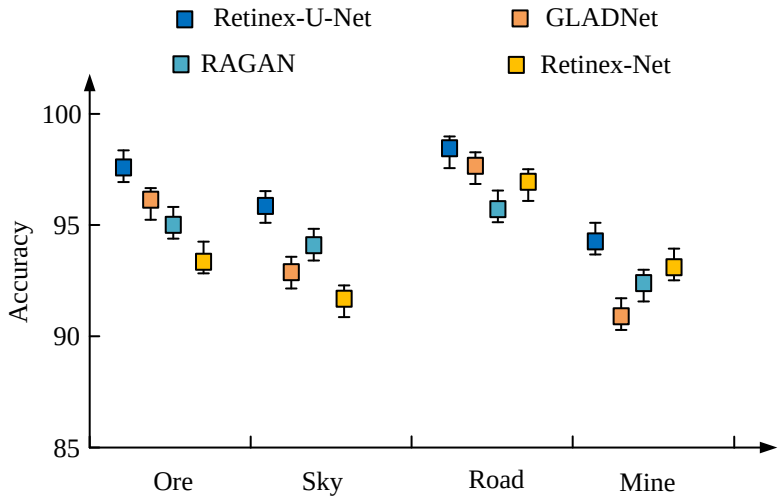

Figure 12: Enhancement performance of items in different mining areas

According to Figure 12, the image enhancement accuracy for ore, sky, mining road, and mining cave is 97, 95, 98, and 94 for the Retinex-U-Net model, respectively, with 96, 92, 97, and 91 for GLADNet model, 95, 94, 96, and 92 for RAGAN model, and 96, 92, 97, and 93 for Retinex-Net model. The data demonstrate that the designed model has good enhancement performance for various objects in the mining area. The comprehensive performance of each model is compared, and the results are shown in Table 2.

Table 2: Comprehensive performance comparison of models

Type	Retinex-Net			GLADNet			RAGAN			Retinex-U-Net		
	ACC	RMSE	Time(s)	ACC	RMSE	Time(s)	ACC	RMSE	Time(s)	ACC	RMSE	Time(s)
Data set 1	77.6	35.7	0.82	81.7*	29.6*	0.69*	89.1*	11.1*	0.57*	94.1**	7.1**	0.49**
Data set 2	78.9	37	0.76	83.2*	27.1*	0.63*	90.5*	12.4*	0.51*	96.6**	8.4**	0.43**
Data set 3	75.8	32.7	0.88	78.6*	22.6*	0.75*	85.8*	7.8*	0.63*	92.7**	3.9**	0.51**
Data set 4	67.7	24.7	0.97	71.9*	14.8*	0.84*	77.9*	4.7*	0.64*	85.4**	2.1**	0.52**
Data set 5	79.2	35.9	1.24	82.7*	25.6*	0.85*	88.7*	9.5*	0.65*	94.5**	3.7**	0.53**

Note: Compared with the Retinex-Net model, * represents P<0.05, and ** represents P<0.01.

According to Table 2, the recognition rates of each model for datasets 4 and 6 are poor, but the proposed Retinex-U-Net model still performs well in the four algorithm models. Compared to the Retinex-Net model, each model shows significant differences in performance (P<0.05). Table 3 shows the details, with 10 individuals selected from 5 groups to assess the performance.

Table 3: User rating table

/	Group 1	Group 2	Group 3	Group 4	Group 5
Retinex-U-Net	92	97	95	84	87
GLADNet	87	82	81	79	81
RAGAN	85	85	79	75	78
Retinex-Net	80	76	78	73	76

In Table 3, the ratings of different models for five groups are 92, 97, 95, 84, and 87 for the Retinex-U-Net model, with 87, 82, 81, 79, and 81 for GLADNet, 85, 85, 79, 75, and 78 for RAGAN, and 80, 76, 78, 73, and 76 for Retinex-Net. The results indicate that the Retinex-U-Net model has a good rating, indicating that it is more favored by users.

5 Discussion

This study proposes a visual IEA for coal mine exploration robots based on Retinex. The method first decomposes LII into illumination maps and reflection maps through the illumination smoothing LF. Then, by improving Retinex-Net, the illumination maps are enhanced and the reflection maps are denoised. Finally, the two are combined to output the enhanced image. The experimental results show that as the validation set increases, except for the improved Retinex-Net algorithm, the SSIM values of all three models decrease with the increase of the validation set. The improved Retinex-Net algorithm does not show significant changes with the increase of the validation set. This is due to the fact that, with the exception of the Retinex-Net model, other models are unable to analyze data effectively when dealing with large datasets, which consequently results in a decrease in their performance. The RMSE values of the four algorithms decrease with the increase of iteration times, among which the RMSE value of the improved Retinex-Net algorithm decreases the most. This is because the improved Retinex-Net model can more fully extract information from the data and integrate it together. In both datasets, the performance of the four models declines with the expansion of the dataset. However, the Retinex-U-Net model demonstrates a minimal decline in performance with the enlargement of the experimental set, maintaining a high level of efficacy. This is due to the Retinex-U-Net model's robust generalization capacity and its ability to process large datasets.

6 Conclusion

Nowadays, with the continuous advancement of coal mine exploration technology, coal mine exploration robots have been widely used in the field of mining exploration and monitoring. However, due to the unique nature of coal mining environments, robots often encounter problems such as uneven illumination and low contrast in images obtained in complex mine environments. This severely limits the clarity and usability of the image. In response to this issue, this study proposed a visual IEA for coal mine exploration robots based on Retinex. This algorithm could enhance LII to obtain information in the images. The experiment showed that when the training set reached 1000, the SSIM values

of improved Retinex-Net, GLADNet, RAGAN, and Retinex-Net were 0.98, 0.95, 0.89, and 0.88, respectively. When the number of iterations reached 250, the LF values of the above four methods were 1.8, 1.5, 1.2, and 0.8, respectively. Selecting common items in the mining area to enhance them, the Retinex-U Net model had image enhancement accuracy of 97, 95, 98, and 94 for ore, sky, mining road, and mining cave, respectively. Selecting users to evaluate the model, and the five groups rated the Retinex-U-Net model at 92, 97, 95, 84, and 87, respectively. The research results indicated that the proposed model had better model performance compared to other models. However, there are still shortcomings in this study, as the data used is relatively single. Subsequent research can integrate sensor data from the mining environment into the image enhancement process. The integration of data from light sensors, thermal imaging cameras, or other environmental sensors enables future models to dynamically adjust their parameters in response to changes in illumination conditions. This capability allows the model to maintain optimal image quality even in highly dynamic environments.

7 Funding

The research was supported by the Natural Science Foundation of the Anhui Higher Education Institutions of China "Research on the Construction of Land Quality Survey and Evaluation Model for Typical Yangtze River Main Stream Based on Remote Sensing Technology" (No. 2022AH040337).

References

[1] M. Adamski, K. Sarnacki, and K. Saeed, “Binary handwriting image enhancement by directional field-guided morphology,” Information Sciences, vol. 551, no. 23, pp.168-183, 2021. https://doi.org/10.1016/j.ins.2020.11.019

[2] L. He, W. Long, S. Liu, Y. Li, and W. Ding, “A night low-illumination image enhancement model based on small probability area filtering and lossless mapping enhancement,” IET Image Processing, vol. 15, no. 13, pp. 3221-3238, 2021. https://doi.org/10.1049/ipr2.12319

[3] Y. Fu, Y. Hong, L. Chen, and S. You, “LE-GAN: Unsupervised low-light image enhancement network using attention module and identity invariant loss,” Knowledge-Based Systems, vol. 24, no, 15, pp. 240-251, 2022. https://doi.org/10.1016/j.knosys.2021.108010

[4] Y. Xu, C. Yang, B. Sun, X. Yan, and M. Chen, “A novel multi-scale fusion framework for detail-preserving low-light image enhancement,” Information Sciences, vol. 548, no. 12, pp. 378-397, 2021. https://doi.org/10.1016/j.ins.2020.09.066

[5] G. Zhou, L. He, Y. Qi, M. Yang, X. Zhao, and Y. Chao, “An improved algorithm using weighted guided coefficient and union self-adaptive image enhancement for single image haze removal,” IET Image Processing, vol. 15, no. 11, pp. 2680-2692, 2021. https://doi.org/10.1049/IPR2.12255

[6] K. He, D. Tao, and D. Xu, “Adaptive colour restoration and detail retention for image enhancement,” IET Image Processing, vol. 15, no. 14, pp. 3685-3697, 2021. https://doi.org/10.1049/ipr2.12223

[7] H. Zhang, W. Qian, M. Wan, and K. Zhang, “Infrared image enhancement algorithm using local entropy mapping histogram adaptive segmentation,” Infrared Physics and Technology, vol. 120, no. 12, pp. 231-248, 2022. https://doi.org/10.1016/j.infrared.2021.104000

[8] B. Lu, Z. Pang, Y. Gu, and Y. Zheng, “Channel splitting attention network for low-light image enhancement,” IET Image Processing, vol. 17, no. 1, pp. 1403-1414, 2022. https://doi.org/10.1049/ipr2.12418

[9] H. H. Yang, K. C. Huang, and W. T. Chen, “LAFFNet: A lightweight adaptive feature fusion network for underwater image enhancement,” IET Image Processing, vol. 3, no. 2, pp. 774-785, 2021. https://doi.org/10.1109/ICRA48506.2021.9561263

[10] D. Wang, R. Lai, and J. Guan, “Target attention deep neural network for infrared image enhancement,” Infrared Physics & Technology, vol. 115, no. 12, pp. 1036-1051, 2021. https://doi.org/10.1016/j.infrared.2021.103690

[11] Q. Jiang, Y. Zhang, F. Bao, and P. Liu, “Two-step domain adaptation for underwater image enhancement,” Pattern Recognition, vol. 122, no. 208, pp. 1083-1092, 2021. https://doi.org/10.1016/j.patcog.2021.108324

[12] H. Zhang, L. Sun, L. Wu, and K. Gu, “DuGAN: An effective framework for underwater image enhancement,” IET Image Processing, vol. 15, no. 9, pp. 1254-1265, 2021. https://doi.org/10.1049/ipr2.12172

[13] X. Chen, J. Li, and Z. Hua, “Low-light image enhancement based on exponential Retinex variational model,” IET Image Processing, vol. 15, no. 12, pp. 1347-1351, 2021. https://doi.org/10.1049/ipr2.12287

[14] D. Zhu, Z. Liu, and Y. Zhang, “Underwater image enhancement based on colour correction and fusion,” IET Image Processing, vol. 15, no. 4, pp. 177-187, 2021. https://doi.org/10.1049/ipr2.12247

[15] F. Katrcolu, “Colour image enhancement with brightness preservation and edge sharpening using a heat conduction matrix,” IET Image Processing, vol. 14, no. 13, pp. 3202-3214, 2020. https://doi.org/10.1049/iet-ipr.2020.0393

[16] F. Janan, and M. Brady, “RICE: A method for quantitative mammographic image enhancement,” Medical Image Analysis, vol. 71, no. 2, pp. 255-268, 2021. https://doi.org/10.1016/j.media.2021.102043

[17] T. Maehata, A. Fujimoto, T. Uraoka, M. Kato, and N.

Yahagi, “Efficacy of a new image enhancement technique for achieving hemostasis in endoscopic submucosal dissection,” Gastrointestinal Endoscopy, vol. 92, no. 3, pp. 541-560, 2020. https://doi.org/10.1016/j.gie.2020.05.033

[18] M. Szabó, “Building ensemble models with web services on microservice architecture,” Informatica, vol. 48, no. 7, pp. 12-17, 2024. https://doi.org/10.31449/inf.v48i7.4918

[19] Y. Yang, and X. Song, “Research on face intelligent perception technology integrating deep learning under different illumination intensities,” Journal of Computational and Cognitive Engineering, vol. 1, no. 1, pp. 32-36, 2022. https://doi.org/10.47852/bonviewJCCE19919